Phosphorus–Carbon Bond Cleavage and Tetrahedrane Cluster Activation in the Reaction between Bis(diphenylphosphino)maleic Anhydride (BMA) and $PhCCo_3(CO)_9$. Syntheses, Kinetic Studies, and X-ray Diffraction Structures of $PhCCo_3(CO)_7$(bma) and $Co_3(CO)_6(\mu_2\text{-}\eta^2,\eta^1\text{-}C(Ph)C{=}C(PPh_2)C(O)OC(O))(\mu_2\text{-}PPh_2)$

Kaiyuan Yang, Janna M. Smith, Simon G. Bott,* and Michael G. Richmond*

Center for Organometallic Research and Education, Department of Chemistry, University of North Texas, Denton, Texas 76203

Received July 6, 1993®

The tricobalt cluster $PhCCo_3(CO)_9$ (1) reacts with the bidentate phosphine ligand 2,3-bis(diphenylphosphino)maleic anhydride (bma) in the presence of added Me_3NO to give the diphosphine-substituted cluster $PhCCo_3(CO)_7$(bma) (2). Cluster 2 is unstable in solution, readily losing CO to afford $Co_3(CO)_6(\mu_2\text{-}\eta^2,\eta^1\text{-}C(Ph)C{=}C(PPh_2)C(O)OC(O))(\mu_2\text{-}PPh_2)$ (3) as the sole observed product. Both clusters have been isolated and characterized by IR and NMR (^{31}P and ^{13}C) spectroscopy. Variable-temperature ^{31}P NMR measurements on cluster 2 indicate that the bma ligand functions as both a bridging and a chelating ligand. At −97 °C, ^{31}P NMR analysis of 2 reveals a K_{eq} of 5.7 in favor of the bridged bma cluster. The bridged bma cluster 2 is the only observed species above −50 °C. Clusters 2 and 3 have been structurally characterized by single-crystal X-ray diffraction analyses. 2 crystallizes in the orthorhombic space group $Pna2_1$: a = 20.488(2) Å, b = 10.620(1) Å, c = 17.665(1) Å, V = 3844 Å^3, Z = 4, d_{calc} = 1.604 g·cm^{-3}; R = 0.0367, R_w = 0.0391 for 1344 observed reflections. 3 crystallizes in the monoclinic space group $P2_1/n$: a = 11.538(1) Å, b = 17.0754(8) Å, c = 19.506(1) Å, β = 92.108(7)°, V = 3840 Å^3, Z = 4, d_{calc} = 1.557 g·cm^{-3}; R = 0.0392, R_w = 0.0432 for 2012 observed reflections. The solid-state structure of 2 does not correspond to the major bridging isomer observed in solution but rather the minor chelating isomer. The presence of the new six-electron $\mu_2\text{-}\eta^2,\eta^1$-benzylidene(diphenylphosphino)maleic anhydride ligand in 3, which results from the coupling of the μ_3-benzylidyne capping group in 2 with the bma ligand, is established by X-ray crystallography. The conversion of 2 to 3 followed first-order kinetics, with the reaction rates being independent of the nature of the reaction solvent and strongly suppressed by added CO, supporting dissociative CO loss as the rate-determining step. The activation parameters for CO loss were determined to be $\Delta H^{\ddagger}$ = 29.9 ± 2.2 kcal/mol and $\Delta S^{\ddagger}$ = 21 ± 6 eu. The reactivity of 2 in the cleavage of the olefinic phosphorus–carbon bond relative to the analogous diphosphine-substituted cluster $PhCCo_3(CO)_7$(*cis*-$Ph_2PCH{=}CHPPh_2$) is discussed, and plausible mechanisms for the chelate to bridge bma ligand exchange in 2 and the formation of cluster 3 are presented.

Introduction

The use of ancillary phosphine ligands in catalytic hydrogenation and hydroformylation reactions has been extensively studied.[1,2] Altered product distributions and increased catalyst stability are cited as two major reasons for the use of phosphine-substituted complexes.[3,4] Implicit with the use of these phosphine-modified catalysts has been the assumed stability of the metal–phosphine complex, which in selected cases of mononuclear complexes and to a greater extent polynuclear complexes has been proven invalid. For example, both cyclometalation and phosphorus–carbon bond cleavage reactions are well-documented pathways available to organometallic phosphine complexes.[5–8] The latter pathway is responsible for catalyst deactivation in certain cobalt-catalyzed hydroformylation reactions.[9,10]

We recently examined the reaction between $PhCCo_3(CO)_9$ (1) and the bidentate phosphine ligand 2,3-bis-

• Abstract published in *Advance ACS Abstracts*, October 15, 1993.

(1) (a) *Homogeneous Catalysis With Metal Phosphine Complexes*; Pignolet, L. H., Ed.; Plenum Press: New York, 1983. (b) Collman, J. P.; Hegedus, L. S.; Norton, J. R.; Finke, R. G. *Principles and Applications of Organotransition Metal Chemistry*; University Science Books: Mill Valley, CA, 1987.

(2) (a) Kagan, H. B. *Bull. Soc. Chim. Fr.* **1988**, 846. (b) Noyori, R.; Takayi, H. *Acc. Chem. Res.* **1990**, *23*, 345. (c) Zassinovich, G.; Mestroni, G.; Gladiali, S. *Chem. Rev.* **1992**, *92*, 1051. (c) Halpern, J. *Science* **1982**, *217*, 401.

(3) (a) Pruett, R. L. *Adv. Organomet. Chem.* **1979**, *17*, 1. (b) Slaugh, L. H.; Mullineaux, R. D. *J. Organomet. Chem.* **1968**, *13*, 469. (c) Crabtree, R. A. *The Organometallic Chemistry of the Transition Metals*; Wiley: New York, 1988. (d) Masters, C. *Homogeneous Transition-Metal Catalysis*; Chapman and Hall: New York, 1981.

(4) (a) Don, M.-J.; Richmond, M. G. *J. Mol. Catal.* **1992**, *73*, 181. (b) Collin, J.; Jossart, C.; Balavoine, G. *Organometallics* **1986**, 203.

(5) Lavigne, G. In *The Chemistry of Metal Cluster Complexes*; Shriver, D. F., Kaesz, H. D., Adams, R. D., Eds.; VCH: New York, 1990; Chapter 5.

(6) Abatjoglou, A. G.; Billig, E.; Bryant, D. R.; Nelson, J. R. *ACS Symp. Ser.* **1992**, *486*, 229.

(7) Harley, A. D.; Guskey, G. J.; Geoffroy, G. L. *Organometallics* **1983**, *2*, 53.

(8) (a) Garrou, P. E. *Chem. Rev.* **1985**, *85*, 171. (b) Garrou, P. E.; Dubois, R. A.; Jung, C. W. *CHEMTECH* **1985**, *15*, 123.

(9) Dubois, R. A.; Garrou, P. E.; Lavin, K. D.; Allcock, H. R. *Organometallics* **1986**, *5*, 460.

(10) Dubois, R. A.; Garrou, P. E. *Organometallics* **1986**, *5*, 466.

0276-7333/93/2312-4779$04.00/0

(diphenylphosphino)maleic anhydride (bma) because of our interest in the synthesis and reactivity of polynuclear clusters bearing redox-active phosphine ligands. The bma ligand is unique, on the basis of the work of Fenske[11] and Tyler,[12] who have demonstrated that this ligand assists in the stabilization of mononuclear 19-electron complexes through electron delocalization with the low-lying π^* system of the phosphine ligand. Accordingly, we attempted to prepare the cluster $PhCCo_3(CO)_7(bma)$, which would allow us to examine the redox chemistry and stability of the corresponding one-electron reduction product, $[PhCCo_3(CO)_7(bma)]^{\bullet-}$. The effect of the bma ligand on the redox properties of the cluster can be easily assessed by a comparison with the extensive electrochemical data of known phosphine-substituted $RCCo_3(CO)_7P_2$ clusters.[13] However, when the reaction between $PhCCo_3(CO)_9$ and bma was initially examined in toluene at 75 °C, none of the expected cluster $PhCCo_3(CO)_7(bma)$ was observed, and it was subsequently shown that $Co_3(CO)_6(\mu_2\text{-}\eta^2,\eta^1\text{-}C(Ph)\overline{C{=}C(PPh_2)C(O)OC(O)})(\mu_2\text{-}PPh_2)$ was present. A brief portion of this work has already been communicated.[14]

Herein we report the synthesis and characterization of $PhCCo_3(CO)_7(bma)$ and its conversion to $Co_3(CO)_6(\mu_2\text{-}\eta^2,\eta^1\text{-}C(Ph)\overline{C{=}C(PPh_2)C(O)OC(O)})(\mu_2\text{-}PPh_2)$. The reason for the facile activation of the bma ligand is discussed, and a reactivity comparison is made with the suitable model cluster complex $PhCCo_3(CO)_7(cis\text{-}Ph_2PCH{=}CHPPh_2)$, which is shown to be stable toward $P\text{-}C_{olefin}$ bond cleavage under analogous conditions.

Results

I. Synthesis and Spectroscopic Properties of $PhCCo_3(CO)_7(bma)$. Initially, we examined the reaction between $PhCCo_3(CO)_9$ and bma in toluene at 75 °C in an effort to prepare $PhCCo_3(CO)_7(bma)$. While the conditions chosen were identical to those employed in the synthesis of $PhCCo_3(CO)_7(cis\text{-}Ph_2PCH{=}CHPPh_2)$,[15] the spectral properties (IR and NMR) of the isolated product did not correspond to those of the desired diphosphine cluster $PhCCo_3(CO)_7(bma)$. It was subsequently shown that the product of the thermolysis reaction was the tricobalt cluster $Co_3(CO)_6(\mu_2\text{-}\eta^2,\eta^1\text{-}C(Ph)\overline{C{=}C(PPh_2)C(O)\text{-}OC(O)})(\mu_2\text{-}PPh_2)$ (vide infra). When the same reaction was carried out at 50 °C with monitoring by IR spectroscopy, no intermediates were observed and cluster **3** was again the only observed product. Cluster **2** was considered to be a logical intermediate precursor to cluster **3** on the basis of the many examples of diphosphine-bridged $RCCo_3(CO)_7P_2$ clusters that have been prepared and characterized.[16-19] Therefore, we concentrated our efforts on an alternative synthetic route to cluster **2** since this would allow us to explore the reaction leading to cluster **3**.

Treatment of an equimolar mixture of $PhCCo_3(CO)_9$ and bma with 2 equiv of the oxidative-decarbonylation reagent Me_3NO[20] in either CH_2Cl_2 or THF solution at room temperature led to an immediate reaction, as judged by IR and TLC analyses. Cluster **2** was isolated in 70–80% yield after passage across a short silica gel column. Maximum yields of **2** were obtained by flash-column chromatography at −78 °C using CH_2Cl_2/petroleum ether as the eluting solvent. **2** does not appear to be overly air-sensitive in solution; however, it is extremely temperature sensitive.

The IR spectrum of **2** exhibits two ν(CO) bands at 2065 and 2015 cm^{-1} along with a weak ν(CO) band at 1986 cm^{-1}, which are assignable to terminal cobalt carbonyl groups. The coordinated bma ligand displays two ν(CO) bands at 1824 (w) and 1772 (m) cm^{-1}, representing the vibrationally coupled asymmetric and symmetric carbonyl stretches, respectively.[21] The possibility that these last two assignments may represent μ_2-bridging carbonyl groups was ruled out by the preparation of cluster **2** that was isotopically enriched with ^{13}CO gas. Only the frequencies of the latter two carbonyl bands were unaffected, consistent with their anhydride nature.

Cluster **2** displayed a single, broad resonance at ~δ 37 in the $^{31}P\{^1H\}$ NMR spectrum in THF at room temperature. The presence of only one ^{31}P resonance along with its high-field location suggests that the ancillary bma ligand bridges adjacent cobalt centers. The same sample was next examined at −97 °C in order to reduce the scalar coupling between the ^{31}P and ^{59}Co nuclei. Reduced temperatures effectively serve to shorten the molecular correlation time (τ_c) and have been shown to afford sharper ^{31}P resonances in other phosphine-substituted cobalt clusters.[22] The low-temperature $^{31}P\{^1H\}$ NMR spectrum of **2** revealed the same bridging ^{31}P resonance that was observed at room temperature and the presence of two additional ^{31}P resonances at δ 62 and 54. These latter two resonances are deshielded relative to the bridging bma resonance, making them readily assignable to a chelating bma ligand.[23] The fact that inequivalent ^{31}P resonances are observed indicates that both PPh_2 groups cannot reside in the equatorial plane defined by the cobalt atoms. This is, however, consistent with the presence of a chelating isomer with equatorial and axial PPh_2 groups. Warming this sample to −50 °C led to the disappearance of the chelating ^{31}P resonances and was accompanied by the

(11) (a) Fenske, D.; Becher, H. J. *Chem. Ber.* **1974**, *107*, 117. (b) Fenske, D.; Becher, H. J. *Chem. Ber.* **1975**, *108*, 2115. (c) Fenske, D. *Chem. Ber.* **1979**, *112*, 363.

(12) (a) Mao, F.; Tyler, D. R.; Keszler, D. *J. Am. Chem. Soc.* **1989**, *111*, 130. (b) Mao, F.; Philbin, C. E.; Weakley, T. J. R.; Tyler, D. R. *Organometallics* **1990**, *9*, 1510. (c) Mao, F.; Tyler, D. R.; Rieger, A. L.; Rieger, P. H. *J. Chem. Soc., Faraday Trans.* **1991**, *87*, 3113. (d) Mao, F.; Sur, S. K.; Tyler, D. R. *Organometallics* **1991**, *10*, 419. (e) Tyler, D. R. *Acc. Chem. Res.* **1991**, *24*, 325. (f) Avey, A.; Schut, D. M.; Weakley, T. J. R.; Tyler, D. R. *Inorg. Chem.* **1993**, *32*, 233.

(13) (a) Downard, A. J.; Robinson, B. H.; Simpson, J. *Organometallics* **1986**, *5*, 1132, 1140. (b) Hinkelmann, K.; Heinze, J.; Schacht, H.-T.; Field, J. S.; Vahrenkamp, H. *J. Am. Chem. Soc.* **1989**, *111*, 5078.

(14) Yang, K.; Smith, J. M.; Bott, S. G.; Richmond, M. G. *Inorg. Chim. Acta* **1993**, *212*, 1.

(15) Yang, K.; Bott, S. G.; Richmond, M. G. *J. Organomet. Chem.* **1993**, *454*, 273.

(16) (a) Watson, W. H.; Nagl, A.; Hwang, S.; Richmond, M. G. *J. Organomet. Chem.* **1993**, *445*, 163. (b) Don, M.-J.; Richmond, M. G.; Watson, W. H.; Krawiec, M.; Kashyap, R. P. *J. Organomet. Chem.* **1991**, *418*, 231.

(17) (a) Balavoine, G.; Collin, J.; Bonnet, J. J.; Lavigne, G. *J. Organomet. Chem.* **1985**, *280*, 429. (b) Aime, S.; Botta, M.; Gobetto, R.; Osella, D. *J. Organomet. Chem.* **1987**, *320*, 229.

(18) Downard, A. J.; Robinson, B. H.; Simpson, J. *Organometallics* **1986**, *5*, 1122.

(19) See also: Sutin, K. A.; Kolis, J. W.; Miekuz, M.; Bougeard, P.; Sayer, B. G.; Quilliam, M. A.; Faggiani, R.; Lock, C. J. L.; McGlinchey, M. J.; Jaouen, G. *Organometallics* **1987**, *6*, 439.

(20) (a) Koelle, U. *J. Organomet. Chem.* **1977**, *133*, 53. (b) Albers, M. O.; Coville, N. J. *Coord. Chem. Rev.* **1984**, *53*, 227.

(21) Dolphin, D.; Wick, A. *Tabulation of Infrared Spectral Data*; Wiley-Interscience: New York, 1977.

(22) (a) Schulman, C. L.; Richmond, M. G.; Watson, W. H.; Nagl, A. *J. Organomet. Chem.* **1989**, *368*, 367. (b) Richmond, M. G.; Kochi, J. K. *Organometallics* **1987**, *6*, 254.

(23) Garrou, P. E. *Chem. Rev.* **1981**, *81*, 229 and references therein.

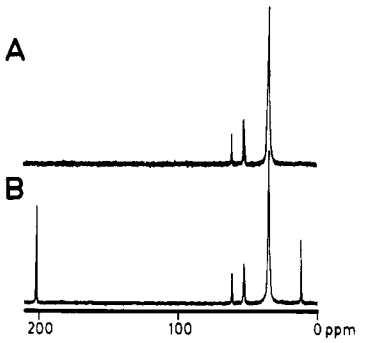

Figure 1. $^{31}P\{^1H\}$ NMR spectra of (A) $PhCCo_3(CO)_7$(bma) before thermolysis at 45 °C and (B) $PhCCo_3(CO)_7$(bma) and $Co_3(CO)_6(\mu_2\text{-}\eta^2,\eta^1\text{-}C(Ph)C{=}C(PPh_2)C(O)OC(O))(\mu_2\text{-}PPh_2)$ after thermolysis at 45 °C. All $^{31}P\{^1H\}$ NMR spectra were recorded at −97 °C in THF.

expected increase in the resonance at δ 37. Cooling the sample back down to −97 °C afforded the original spectrum and demonstrated the reversible nature of the interconversion between the bridging and chelating isomers of cluster **2**. This equilibration process is depicted in eq 1, and a representative $^{31}P\{^1H\}$ NMR spectrum of **2** exhibiting both the bridging and chelating ^{31}P resonances is seen in Figure 1A.

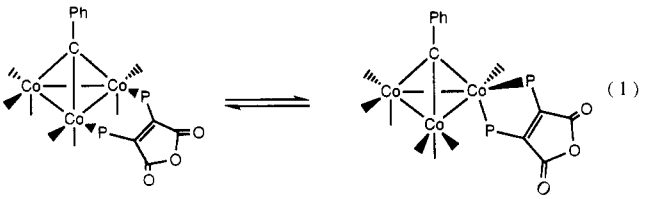

(1)

To our knowledge this bridge/chelate bma ligand equilibration is the first of its kind, and the olefinic bma bond is believed to play a role in the equilibration process on the basis of the absence of similar ^{31}P NMR behavior for the saturated-phosphine cluster $PhCCo_3(CO)_7$(dppe). Here the bridging ^{31}P resonance is the only observed resonance over all temperatures explored.[24] Our concern over the possibility that the chelating isomer may only reflect the existence of a separate and discrete impurity is eliminated by the invariant bridge:chelate ratio measured for different samples of **2**. $^{31}P\{^1H\}$ NMR measurements consistently gave a K_{eq} of ~5.7 in favor of the bridging isomer at −97 °C. Reactivity studies involving the conversion of **2** to **3** also support the proposed temperature-dependent bma ligand equilibration process in **2** (vide infra). Further evidence for this bma ligand equilibration derives from a ^{31}P EXSY study on **2** at −97 °C, which revealed the expected off-diagonal correlations between the bridging and chelating ^{31}P moieties. The full details of this study will be reported in due course.

The solution structure of **2** was also probed by variable-temperature $^{13}C\{^1H\}$ NMR spectroscopy. At −97 °C, three terminal carbonyl resonances at δ 209, 204, and 202 with an integral ratio of 2:2:3, respectively, are observed. Our spectrum is identical to the published NMR spectra for the diphosphine-bridged clusters $PhCCo_3(CO)_7$(dppe)[19] and $PhCCo_3(CO)_7$(*cis*-$Ph_2PCH{=}CHPPh_2$),[15] whose chemical shift assignments and CO-exchange pathways have been thoroughly discussed.[19] The major isomer of **2** in solution by both ^{31}P and ^{13}C NMR spectroscopy clearly possesses an equatorially disposed bridging bma ligand. Besides these three major carbonyl resonances, a small resonance at ~δ 207 is seen and assigned to the minor chelating bma isomer of **2**. The presence of only one carbonyl resonance for this isomer may indicate that intramolecular CO exchange is still rapid at −97 °C, conditions which would give rise to the single observed resonance. Alternatively, the other carbonyl groups of **2** (chelated) may be obscured by the CO groups associated with the bridged isomer of **2**. While we cannot distinguish between these two possibilities at this point, we favor the former explanation since it is known that CO scrambling is, as a rule of thumb, generally faster than that of phosphine-ligand scrambling.[19,22b] The low-temperature ^{13}C NMR spectrum of **2** is shown in Figure 2A.

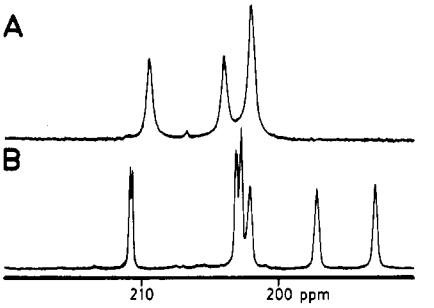

Figure 2. $^{31}C\{^1H\}$ NMR spectra of (A) $PhCCo_3(CO)_7$(bma) and (B) $Co_3(CO)_6(\mu_2\text{-}\eta^2,\eta^1\text{-}C(Ph)C{=}C(PPh_2)C(O)OC(O))(\mu_2\text{-}PPh_2)$ recorded at −97 °C in THF.

As the temperature is raised to −50 °C, the carbonyl resonances broaden, more or less at the same rate, and merge to give a single, broad resonance at δ 205, which is in agreement with the weighted-average chemical shift for the bridging isomer of **2**. Further warming to room temperature leads to a slight sharpening of the resonance at δ 205. This NMR behavior is fully reversible, as evidenced by repeated cooling and warming cycles. The ^{13}C NMR observation of bma-bridged **2** as the major isomer in solution is consistent with the reported ^{31}P NMR data, and the dynamic NMR behavior underscores the extreme ease with which the ancillary bma and CO groups interconvert in solution.

II. Synthesis and Spectroscopic Properties of $Co_3(CO)_6(\mu_2\text{-}\eta^2,\eta^1\text{-}C(Ph)C{=}C(PPh_2)C(O)OC(O))(\mu_2\text{-}PPh_2)$. Cluster **2** readily loses CO and transforms to cluster **3** upon gentle heating in a variety of solvents. These thermolysis reactions unequivocally establish the intermediacy of diphosphine **2** in the formation of **3** and allow the overall reaction to be delineated as illustrated in eq 2. The inability to observe cluster **2** in the thermolysis

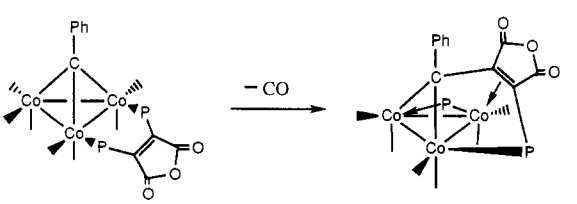

(2)

reactions involving $PhCCo_3(CO)_9$ and bma provides an important view of the relative rates of formation for clusters **2** and **3**. Starting from cluster $PhCCo_3(CO)_9$, the observation of cluster **2** is not expected if the subsequent reactions leading to **3** all occur at faster rates. Independent

(24) Unpublished variable-temperature ^{31}P NMR results. See ref 18 for the room-temperature ^{31}P chemical shift of $PhCCo_3(CO)_7$(dppe).

kinetic measurements that confirm this scenario are discussed in the next section.

Cluster **3** was isolated by chromatography over silica gel using CH_2Cl_2 solvent and characterized spectroscopically in solution. The IR spectrum displays terminal carbonyl stretching bands at 2062 (m), 2042 (vs), 2025 (vs), 2010 (s), and 1939 (m) cm^{-1} along with the characteristic bma carbonyl bands at 1811 and 1749 cm^{-1}. As with the precursor cluster, **2**, these two bands are assigned to the asymmetric and symmetric ν(C=O) modes of the anhydride moiety.[21] The $^{31}P\{^1H\}$ NMR spectrum of **3** showed a pair of equal-intensity resonances at δ 201 and 12, which are attributed to a μ_2-phosphido and a coordinated Co–PR_3 group, respectively. A ^{13}CO-enriched sample of **3** was prepared, and the $^{13}C\{^1H\}$ NMR spectrum was recorded at −97 °C to reduce the undesired quadrupolar broadening between the Co and CO nuclei. The resulting spectrum exhibited six equal-intensity resonances, as shown in Figure 2B. Of these resonances, the two downfield resonances centered at δ 210.5 and 202.9 reveal phosphorus coupling and J_{P-C} values of 12.3 and 7.9 Hz, respectively. No attempt has been made to assign these resonances to a specific CO group. The observation of six CO groups supports the static structure of **3** shown in eq 2. In comparison to **2**, which exhibits dynamic ligand behavior, **3** maintains a static structure over the temperature range of −97 °C to room temperature.

We have also studied the conversion of **2** to **3** by ^{31}P NMR spectroscopy as a way to establish the equilibrium between the chelating and bridging forms of **2**. The −97 °C $^{31}P\{^1H\}$ NMR spectrum of a 0.034 M THF solution of **2** was initially examined before the thermolysis reaction. The spectrum is shown in Figure 1a, and as discussed, a K_{eq} value of ~5.7 in favor of the bridged-bma isomer was calculated. The sample was next removed from the spectrometer probe and placed in a temperature-controlled bath at 45 °C for a period of time sufficient to effect partial conversion to cluster **3**. After quenching of the reaction in a dry ice/acetone bath, the ^{31}P NMR spectrum was recorded again at −97 °C. The resulting spectrum, which is shown in Figure 1B, reveals the presence of cluster **3**, on the basis of the resonances at δ 201 and 12, and cluster **2**. More importantly, the ratio of the bridging and chelating isomers of **2** remained unchanged relative to that of the initial spectrum, evidence which supports a facile equilibrium between these two isomers.

III. Kinetic Study on the Conversion of 2 to 3. The kinetics for the reaction of **2** to **3** were investigated by IR spectroscopy in THF solution over the temperature range 27–57 °C. The reaction followed first-order kinetics over a period of 2–3 half-lives, and the reported first-order rate constants, which are quoted in Table I, were calculated by monitoring the absorbance decrease in the bma band at 1772 cm^{-1} of **2**. Changing the solvent from THF to either CH_2Cl_2 or 2,5-Me_2THF (entries 3 and 6) did not affect the rate of the reaction, but the introduction of CO (1 atm) resulted in a sharp retardation in the rate. Entries 2 and 4 allow for a direct comparison of the effect of CO on this reaction. The presence of CO slows the formation of cluster **3** by a factor of ~36. These data suggest that the rate-determining step is best described by a unimolecular mechanism involving dissociative CO loss, as outlined in eq 3. Treating the unsaturated intermediate $PhCCo_3(CO)_6$(bma) (**e**) within the steady-state approximation

Table I. Experimental Rate Constants for the Reaction of $PhCCo_3(CO)_7$(bma) (2) Leading to $Co_3(CO)_6(\mu_2\text{-}\eta^2,\eta^1\text{-}C(Ph)C{=}(PPh_2)C(O)OC(O))(\mu_2\text{-}PPh_2)$ (3)[a]

entry no.	T, °C	$10^5 k_{obsd}$,[b] s^{-1}	entry no.	T, °C	$10^5 k_{obsd}$,[b] s^{-1}
1	27.0	3.7 ± 0.8	5	43.6	63 ± 6
2	34.2	18.10 ± 0.02	6[e]	43.6	63 ± 9
3[c]	34.2	20 ± 1	7	50.2	185 ± 24
4[d]	34.2	0.51 ± 0.06	8	57.0	368 ± 18

[a] From ~8.2×10^{-3} M $PhCCo_3(CO)_7$(bma) in THF by following the disappearance of the 1772-cm^{-1} IR band. All THF kinetic data quoted represent the average of two measurements. [b] Error limits at the 95% confidence level. [c] CH_2Cl_2 used as solvent. [d] In the presence of 1 atm of CO. [e] 2,5-Me_2THF used as solvent.

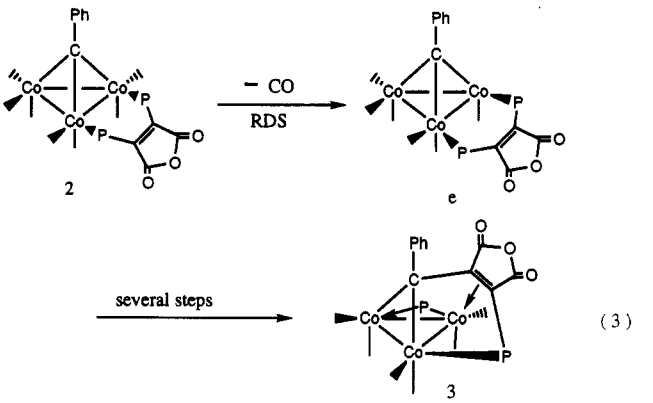

(3)

affords the rate law

$$\text{rate} = \frac{k_1 k_2[PhCCo_3(CO)_7(bma)]}{k_{-1}[CO] + k_2}$$

which, in the absence of added CO ($k_2 > k_{-1}$[CO]), reduces to rate = $k_1[PhCCo_3(CO)_7(bma)]$, as expected for a dissociation mechanism. The observed CO inhibition and the activation parameters $\Delta H^{\ddagger}$ = 29.9 ± 2.2 kcal/mol and $\Delta S^{\ddagger}$ = 21 ± 6 eu are fully consistent with the proposed mechanism. We wish to point out that this mechanism does not give us any information concerning the timing of the P–C bond cleavage of the bma ligand and formation of the μ_2-η^2,η^1-benzylidene(diphenylphosphino)maleic anhydride ligand because these steps occur after the rate-determining step. However, we do know that the lower limit for the rate of these steps cannot be less than the reported rates in Table I. Future kinetic studies will be directed toward the extraction of the rate constants of these reactions using transient spectroscopic measurements.

IV. X-ray Diffraction Structures of $PhCCo_3(CO)_7$(bma) and $Co_3(CO)_6(\mu_2\text{-}\eta^2,\eta^1\text{-}C(Ph)C{=}C(PPh_2)C(O)OC(O))(\mu_2\text{-}PPh_2)$. Single crystals of **2** and **3** were grown, and the molecular structure of each cluster was determined. Both clusters exist as discrete molecules in the unit cell with no unusually short inter- or intramolecular contacts. The X-ray data collection and processing parameters for **2** and **3** are given in Table II with the final fractional coordinates listed in Table III. The ORTEP diagrams in Figure 3 show the molecular structure of each cluster and establish the disposition of the bma ligand in **2** and the presence of the six-electron μ_2-η^2,η^1-benzylidene(diphenylphosphino)maleic anhydride and the μ_2-phosphido ligands in **3**. Selected bond distances and angles are given in Table IV.

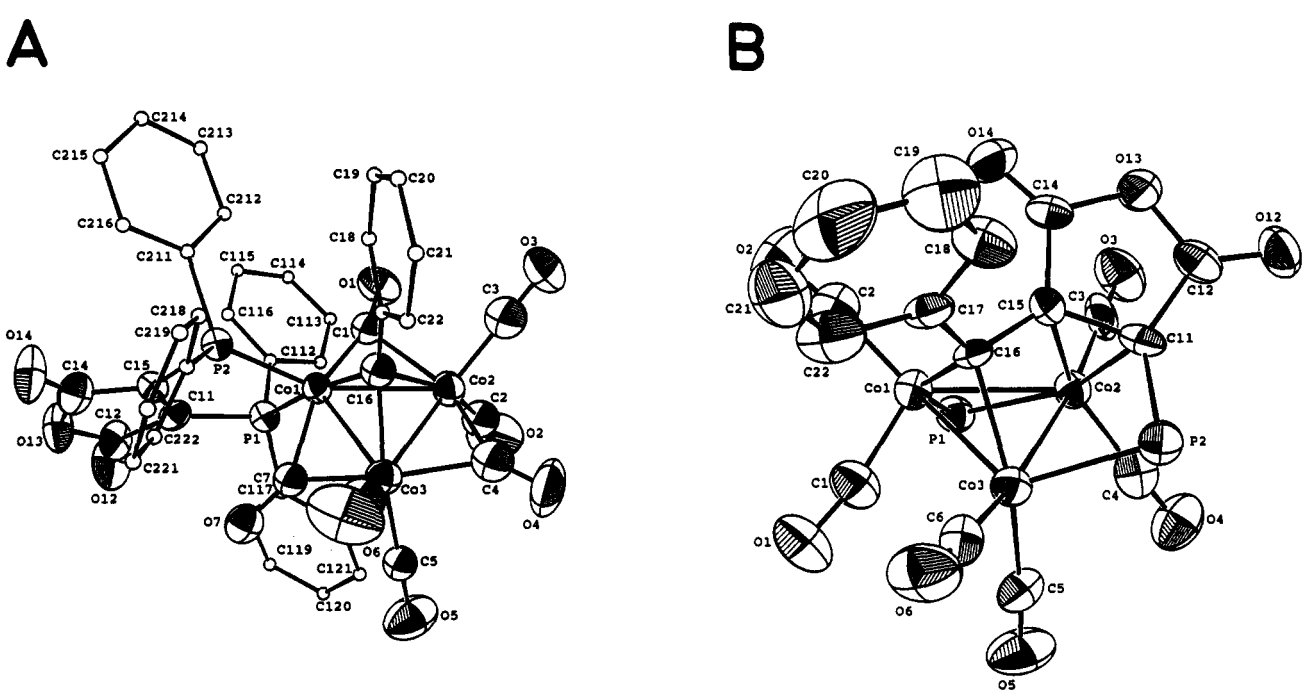

Figure 3. ORTEP drawings of the non-hydrogen atoms of (A) $PhCCo_3(CO)_7$(bma) and (B) $Co_3(CO)_6(\mu_2\text{-}\eta^2,\eta^1\text{-}C(Ph)C{=}C(PPh_2)C(O)OC(O))(\mu_2\text{-}PPh_2)$. Thermal ellipsoids are drawn at the 50% probability level.

Table II. X-ray Crystallographic Data for the Tricobalt Clusters 2 and 3

	2	3
space group	$Pna2_1$, orthorhombic (No. 33)	$P2_1/n$, monoclinic (No. 14)
a, Å	20.488(2)	11.538(1)
b, Å	10.620(1)	17.0754(8)
c, Å	17.665(1)	19.506(1)
β, deg		92.108(7)
V, Å^3	3843.8(9)	3840.4(7)
mol formula	$C_{42}H_{25}Co_3O_{10}P_2$	$C_{41}H_{25}Co_3O_9P_2$
fw	928.41	900.40
formula units per cell (Z)	4	4
ρ, g·cm^{-3}	1.604	1.557
abs coeff (μ), cm^{-1}	14.17	14.14
λ(Mo Kα), Å	0.710 73	0.710 73
collecn range, deg	$2.0 \le 2\theta \le 40.0$	$2.0 \le 2\theta \le 44.0$
max scan time, s	120	120
scan speed range, deg·min^{-1}	0.67–8.0	0.67–8.0
tot. no. of data collcd	2080	5169
no. of indep data	2080	4898
no. of indep data, $I > 3\sigma(I)$	1344	2012
R	0.0367	0.0392
R_w	0.0391	0.0432
weights	$[0.04F^2 + (\sigma(F)^2]^{-1}$	$[0.04F^2 + (\sigma(F)^2]^{-1}$

Cluster **2** possesses a chelating bma ligand and bridging carbonyl groups in the solid state. Several attempts to crystallize the bridging isomer of **2** were made, but these were not successful and only the chelating isomer was observed. Additional proof concerning the preference of **2** to adopt a chelating bma ligand with bridging CO groups in the solid state is seen in the IR spectrum (KBr) of **2**, where an intense bridging CO band at 1855 cm^{-1} is observed. We also note that this same band is not present in solution as a result of rapid bma/CO ligand fluxionality which serves to give the chelated isomer of **2** with rapidly exchanging carbonyl groups and the bridged isomer of **2**.

The polyhedral core of **2** consists of a triangular array of cobalt atoms capped by a μ_3-CPh moiety. Unequal Co–Co bond lengths are seen in **2**, with the bma-substituted Co–Co bonds being 0.094 Å longer than the unique Co(2)–Co(3) bond. We attribute this to a sterically induced perturbation of the cluster by the bma ligand. The mean value for the μ_3-C–Co (1.94 Å) and the Co–CO (1.76 Å) distances are consistent with those reported for related clusters.[25] The remaining distances and angles are unexceptional and require no comment.

The Co–Co bond distances in cluster **3** range from 2.412(2) to 2.696(2) Å while a mean distance of 2.197 Å is observed for the μ_2-P–Co bonds. The μ_2-P–Co distances found are in good agreement with those of other phosphido-bridged cobalt clusters.[26] All other bond lengths and angles are within normal limits and require no comment.

Discussion

The reaction of $PhCCo_3(CO)_9$ with the bidentate phosphine bma proceeds initially to give the diphosphine cluster

(25) (a) Colbran, S. B.; Robinson, B.; Simpson, J. *Acta Crystallogr.* **1986**, *C42*, 972. (b) Ahlgrén, M.; Pakkanen, T. T.; Tahvanainen, I. *J. Organomet. Chem.* **1987**, *323*, 91. (c) Aitchison, A. A.; Farrugia, L. J. *Organometallics* **1987**, *6*, 819. (d) Brice, M. D.; Penfold, B. R.; Robinson, W. T.; Taylor, S. R. *Inorg. Chem.* **1970**, *9*, 362.

Table III. Positional Parameters for Non-Hydrogen Atoms of the Tricobalt Clusters 2 and 3 with Estimated Standard Deviations in Parentheses[a]

atom	*x*	*y*	*z*	*B*, Å²	atom	*x*	*y*	*z*	*B*, Å²
				$PhCCo_3(CO)_7$(bma) (**2**)					
Co(1)	0.65275(9)	0.2201(2)	0.772	2.53(3)	C(19)	0.4260(8)	0.181(1)	0.6862(9)	4.8(4)*
Co(2)	0.61469(9)	0.0145(2)	0.8257(1)	3.42(4)	C(20)	0.4098(8)	0.101(2)	0.628(1)	5.1(4)*
Co(3)	0.68234(9)	0.0126(2)	0.7140(1)	3.28(4)	C(21)	0.4550(9)	0.017(2)	0.600(1)	6.5(5)*
P(1)	0.7241(2)	0.3463(3)	0.8318(2)	2.72(8)	C(22)	0.5174(8)	0.015(2)	0.6317(9)	4.7(4)*
P(2)	0.6288(2)	0.3720(3)	0.6923(2)	2.62(8)	C(111)	0.6943(7)	0.430(1)	0.9128(8)	3.2(3)*
O(1)	0.5709(5)	0.254(1)	0.9060(5)	4.8(3)	C(112)	0.6953(8)	0.374(2)	0.982(1)	4.7(4)*
O(2)	0.6827(6)	−0.030(1)	0.9683(7)	7.8(4)	C(113)	0.665(1)	0.426(2)	1.046(1)	6.9(5)*
O(3)	0.4812(5)	−0.062(1)	0.8531(8)	6.9(3)	C(114)	0.6379(9)	0.540(2)	1.037(1)	6.5(5)*
O(4)	0.6437(6)	−0.2379(9)	0.7702(9)	7.1(3)	C(115)	0.636(1)	0.603(2)	0.969(1)	7.1(5)*
O(5)	0.8093(5)	−0.100(1)	0.7489(7)	6.8(3)	C(116)	0.6656(8)	0.544(2)	0.906(1)	5.1(4)*
O(6)	0.6673(6)	−0.038(2)	0.5540(7)	8.4(4)	C(117)	0.8023(6)	0.285(1)	0.8639(8)	2.7(3)*
O(7)	0.7739(5)	0.2122(9)	0.6826(5)	4.0(2)	C(118)	0.8530(7)	0.360(1)	0.8886(8)	3.7(3)*
O(12)	0.8314(5)	0.604(1)	0.7937(6)	6.3(3)	C(119)	0.9080(8)	0.300(2)	0.9190(9)	5.0(4)*
O(13)	0.7767(5)	0.6334(9)	0.6866(6)	4.8(3)	C(120)	0.9116(8)	0.173(2)	0.9250(9)	4.8(4)*
O(14)	0.7002(6)	0.622(1)	0.5949(6)	5.7(3)	C(121)	0.8621(8)	0.100(2)	0.903(1)	5.3(4)*
C(1)	0.6023(7)	0.218(1)	0.8557(8)	3.1(3)*	C(122)	0.8066(7)	0.153(1)	0.8711(8)	3.6(3)*
C(2)	0.6556(7)	−0.018(1)	0.9132(9)	4.2(3)*	C(211)	0.5633(6)	0.490(1)	0.7045(8)	3.2(3)*
C(3)	0.5346(7)	−0.030(2)	0.845(1)	4.9(4)*	C(212)	0.5323(7)	0.499(1)	0.7720(9)	4.1(3)*
C(4)	0.6437(8)	−0.130(1)	0.775(1)	4.8(3)*	C(213)	0.4846(8)	0.592(2)	0.783(1)	5.8(4)*
C(5)	0.7593(7)	−0.055(1)	0.7348(8)	3.2(3)*	C(214)	0.4685(9)	0.668(2)	0.725(1)	6.1(4)*
C(6)	0.6734(8)	−0.021(2)	0.6182(9)	4.6(4)*	C(215)	0.4998(8)	0.661(2)	0.658(1)	5.4(4)*
C(7)	0.7241(7)	0.173(1)	0.7102(8)	3.2(3)*	C(216)	0.5478(7)	0.570(1)	0.6446(9)	4.0(3)*
C(11)	0.7385(6)	0.469(1)	0.7587(8)	2.9(3)	C(217)	0.6266(7)	0.332(1)	0.5935(8)	3.0(3)*
C(12)	0.7903(7)	0.572(1)	0.7549(9)	4.0(4)	C(218)	0.5675(7)	0.307(1)	0.5591(8)	3.6(3)*
C(14)	0.7216(8)	0.582(1)	0.6528(9)	4.0(4)	C(219)	0.5633(8)	0.265(2)	0.4847(9)	4.4(4)*
C(15)	0.6987(6)	0.477(1)	0.6997(7)	2.4(3)	C(220)	0.6190(7)	0.248(1)	0.4450(8)	4.0(3)*
C(16)	0.5975(7)	0.094(1)	0.7290(8)	3.2(3)*	C(221)	0.6780(7)	0.273(1)	0.4751(8)	3.5(3)*
C(17)	0.5366(6)	0.099(1)	0.6942(8)	3.1(3)*	C(222)	0.6814(7)	0.316(1)	0.5497(8)	3.3(3)*
C(18)	0.4870(7)	0.177(1)	0.7171(9)	3.9(3)*					
				$Co_3(CO)_6(\mu_2\text{-}\eta^2,\eta^1\text{-}C(Ph)C{=}C(PPh_2)C(O)OC(O))(\mu_2\text{-}PPh_2)$ (**3**)					
Co(1)	0.9763(1)	0.07150(8)	0.26300(7)	2.88(3)	C(20)	0.695(1)	−0.0214(9)	0.4785(6)	7.7(4)
Co(2)	0.8690(1)	0.07212(8)	0.14485(7)	2.71(3)	C(21)	0.794(1)	0.0210(8)	0.4770(6)	6.1(4)
Co(3)	0.8179(1)	0.16346(8)	0.25235(7)	2.80(3)	C(22)	0.836(1)	0.0455(7)	0.4143(6)	5.0(3)
P(1)	1.0615(2)	0.0855(2)	0.1688(1)	3.05(6)	C(111)	1.1279(9)	0.1748(6)	0.1403(5)	3.5(2)*
P(2)	0.6494(2)	0.1325(2)	0.1992(1)	2.94(6)	C(112)	1.200(1)	0.2151(7)	0.1872(6)	5.1(3)*
O(1)	1.0606(7)	0.2053(5)	0.3388(4)	6.2(2)	C(113)	1.252(1)	0.2853(9)	0.1664(8)	7.4(4)*
O(2)	1.0861(7)	−0.0514(5)	0.3436(4)	6.4(2)	C(114)	1.228(1)	0.3150(9)	0.1034(7)	7.2(4)*
O(3)	0.9148(7)	−0.0507(5)	0.0446(4)	5.9(2)	C(115)	1.160(1)	0.2751(8)	0.0567(7)	5.6(3)*
O(4)	0.8332(7)	0.1967(5)	0.0434(4)	5.5(2)	C(116)	1.111(1)	0.2039(7)	0.0753(6)	4.2(3)*
O(5)	0.9083(8)	0.3078(4)	0.1925(5)	6.5(2)	C(117)	1.1528(9)	0.0087(6)	0.1367(5)	3.2(2)*
O(6)	0.7494(8)	0.2304(5)	0.3821(4)	5.9(2)	C(118)	1.243(1)	0.0211(7)	0.0929(6)	4.0(2)*
O(12)	0.5906(6)	−0.0338(4)	0.0878(4)	4.5(2)	C(119)	1.313(1)	−0.0408(7)	0.0730(6)	4.7(3)*
O(13)	0.7196(6)	−0.0952(4)	0.1578(3)	3.7(2)	C(120)	1.293(1)	−0.1141(8)	0.0957(7)	5.7(3)*
O(14)	0.8518(7)	−0.1257(4)	0.2404(4)	4.5(2)	C(121)	1.206(1)	−0.1284(8)	0.1395(7)	5.7(3)*
C(1)	1.018(1)	0.1556(7)	0.3053(6)	4.3(3)	C(122)	1.1341(9)	−0.0668(7)	0.1587(6)	4.2(2)*
C(2)	1.042(1)	−0.0056(7)	0.3086(6)	4.1(3)	C(211)	0.524(1)	0.1118(7)	0.2505(6)	4.1(2)*
C(3)	0.8973(9)	−0.0035(7)	0.0843(5)	3.8(3)	C(212)	0.494(1)	0.1645(7)	0.2998(6)	4.5(3)*
C(4)	0.8461(8)	0.1496(7)	0.0848(5)	3.7(3)	C(213)	0.399(1)	0.1477(8)	0.3427(7)	5.9(3)*
C(5)	0.8707(9)	0.2526(6)	0.2143(6)	3.8(3)	C(214)	0.339(1)	0.0840(8)	0.3304(6)	5.6(3)*
C(6)	0.7757(9)	0.2068(6)	0.3309(5)	3.7(3)	C(215)	0.363(1)	0.0307(8)	0.2818(6)	5.2(3)*
C(11)	0.7054(9)	0.0405(5)	0.1730(5)	2.7(2)	C(216)	0.4569(9)	0.0469(6)	0.2395(6)	4.0(2)*
C(12)	0.6628(8)	−0.0278(6)	0.1334(5)	3.4(3)	C(217)	0.5893(9)	0.1858(6)	0.1268(5)	3.1(2)*
C(14)	0.7949(8)	−0.0768(6)	0.2129(5)	2.6(2)	C(218)	0.608(1)	0.2657(7)	0.1219(6)	4.0(2)*
C(15)	0.7878(8)	0.0088(6)	0.2237(5)	2.8(2)	C(219)	0.563(1)	0.3084(7)	0.0680(6)	5.3(3)*
C(16)	0.8190(8)	0.0518(5)	0.2871(5)	2.7(2)	C(220)	0.500(1)	0.2719(8)	0.0180(6)	5.1(3)*
C(17)	0.778(1)	0.0247(6)	0.3533(5)	3.1(2)	C(221)	0.478(1)	0.1948(7)	0.0207(6)	5.1(3)*
C(18)	0.677(1)	−0.0190(7)	0.3574(6)	4.1(3)	C(222)	0.5233(9)	0.1498(7)	0.0754(5)	3.9(2)*
C(19)	0.635(1)	−0.0426(8)	0.4197(6)	6.1(4)					

[a] Asterisks indicate that atoms were refined isotropically. Anisotropically refined atoms are given in the form of the isotropic equivalent parameter defined as $(4/3)[a^2B(1,1) + b^2B(2,2) + c^2B(3,3) + ab(\cos\gamma)B(1,2) + ac(\cos\beta)B(1,3) + bc(\cos\alpha)B(2,3)]$.

$PhCCo_3(CO)_7$(bma). Variable-temperature ^{31}P NMR measurements indicate that this cluster exists as a mixture of bridged and chelating isomers. At the temperatures examined, the bridged isomer has been found to be the predominant isomer in solution by ^{31}P and ^{13}C NMR spectroscopy. However, X-ray crystallography reveals that the solid-state structure is derived from the chelating isomer.

We believe that the noncoordinated C=C bond of the maleic anhydride ring facilitates the observed bma equilibration process as outlined in Scheme I. Starting with the bridged isomer, **2b**, and invoking a unimolecular mechanism that does not rely on CO loss, we find that phosphine ligand displacement by the maleic anhydride

(26) (a) Albright, T. A.; Kang, S.-K.; Arif, A. M.; Bard, A. J.; Jones, R. A.; Leland, J. K.; Schwab, S. T. *Inorg. Chem.* **1988**, *27*, 1246. (b) Harley, A. D.; Whittle, R. R.; Geoffroy, G. L. *Organometallics* **1983**, *2*, 60. (c) Young, D. A. *Inorg. Chem.* **1981**, *20*, 2049. (d) Baker, R. T.; Calabrese, J. C.; Krusic, P. J.; Therien, M. J.; Trogler, W. C. *J. Am. Chem. Soc.* **1988**, *110*, 8392. (e) Regragui, R.; Dixneuf, P. H.; Taylor, N. J.; Carty, A. J. *Organometallics* **1990**, *9*, 2234.

Table IV. Selected Bond Distances (Å) and Angles (deg) in the Tricobalt Clusters 2 and 3[a]

$PhCCo_3(CO)_7(bma)$ (**2**)

Bond Distances

Co(1)–Co(2)	2.504(3)	Co(1)–Co(3)	2.505(2)
Co(2)–Co(3)	2.411(3)	Co(1)–P(1)	2.247(4)
Co(1)–P(2)	2.198(4)	Co(1)–C(1)	1.80(1)
Co(1)–C(7)	1.89(1)	Co(1)–C(16)	1.91(1)
Co(2)–C(1)	2.24(1)	Co(2)–C(2)	1.79(2)
Co(2)–C(3)	1.74(2)	Co(2)–C(4)	1.88(2)
Co(2)–C(16)	1.94(1)	Co(3)–C(4)	2.02(2)
Co(3)–C(5)	1.77(1)	Co(3)–C(6)	1.74(2)
Co(3)–C(7)	1.91(1)	Co(3)–C(16)	1.96(1)
O(1)–C(1)	1.16(2)	O(2)–C(2)	1.13(2)
O(3)–C(3)	1.15(2)	O(4)–C(4)	1.15(2)
O(5)–C(5)	1.16(2)	O(6)–C(6)	1.16(2)
O(7)–C(7)	1.21(2)	O(12)–C(12)	1.14(2)
O(13)–C(12)	1.40(2)	O(13)–C(14)	1.39(2)
O(14)–C(14)	1.19(2)	C(11)–C(12)	1.53(2)
C(11)–C(15)	1.33(2)	C(14)–C(15)	1.47(2)
C(16)–C(17)	1.39(2)		

Bond Angles

Co(2)–Co(1)–Co(3)	57.53(8)	Co(1)–Co(2)–Co(3)	61.25(7)
Co(1)–Co(3)–Co(2)	61.21(7)	Co(2)–Co(1)–P(1)	123.1(1)
Co(2)–Co(1)–P(2)	144.4(1)	Co(2)–Co(1)–C(1)	60.2(4)
Co(3)–Co(1)–C(7)	48.9(4)	P(1)–Co(1)–P(2)	90.5(1)
P(1)–Co(1)–C(16)	172.0(4)	P(2)–Co(1)–C(16)	97.3(4)
Co(3)–Co(2)–C(4)	54.4(5)	C(2)–Co(2)–C(3)	102.8(7)
C(2)–Co(2)–C(16)	158.4(6)	C(3)–Co(2)–C(16)	96.7(7)
C(5)–Co(3)–C(6)	102.3(7)	C(5)–Co(3)–C(16)	160.2(6)
C(6)–Co(3)–C(16)	97.3(7)	Co(1)–C(1)–O(1)	160(1)
Co(2)–C(1)–O(1)	124(1)	Co(2)–C(2)–O(2)	175(1)
Co(2)–C(3)–O(3)	176(2)	Co(2)–C(4)–Co(3)	76.5(5)
Co(2)–C(4)–O(4)	148(2)	Co(3)–C(4)–O(4)	136(2)
Co(3)–C(5)–O(5)	179(1)	Co(3)–C(6)–O(6)	177(2)
Co(1)–C(7)–Co(3)	82.5(5)	Co(1)–C(7)–O(7)	143(1)
Co(3)–C(7)–O(7)	135(1)		

$Co_3(CO)_6(\mu_2\text{-}\eta^2,\eta^1\text{-}C(Ph)C{=}C(PPh_2)C(O)OC(O))(\mu_2\text{-}PPh_2)$ (**3**)

Bond Distances

Co(1)–Co(2)	2.576(2)	Co(1)–Co(3)	2.412(2)
Co(2)–Co(3)	2.696(2)	Co(1)–C(1)	1.72(1)
Co(1)–C(2)	1.75(1)	Co(1)–C(16)	1.92(1)
Co(2)–P(1)	2.264(3)	Co(2)–C(3)	1.79(1)
Co(2)–C(4)	1.78(1)	Co(2)–C(11)	2.06(1)
Co(2)–C(15)	2.12(1)	Co(3)–P(2)	2.234(3)
Co(3)–C(5)	1.81(1)	Co(3)–C(6)	1.79(1)
Co(3)–C(16)	2.023(9)	C(1)–O(1)	1.17(1)
C(2)–O(2)	1.15(1)	C(3)–O(3)	1.14(1)
C(4)–O(4)	1.15(1)	Co(1)–P(1)	2.129(3)
C(5)–O(5)	1.13(1)	C(6)–O(6)	1.13(1)
C(12)–O(12)	1.20(1)	C(12)–O(13)	1.40(1)
C(14)–O(13)	1.39(1)	C(14)–O(14)	1.18(1)
C(15)–C(16)	1.47(1)	C(11)–C(15)	1.45(1)

Bond Angles

Co(2)–Co(1)–Co(3)	65.34(6)	Co(1)–Co(2)–Co(3)	54.40(5)
Co(1)–Co(3)–Co(2)	60.26(5)	Co(3)–Co(1)–C(16)	54.2(3)
P(1)–Co(1)–C(1)	101.0(4)	P(1)–Co(1)–C(2)	108.6(4)
C(1)–Co(1)–C(2)	106.1(5)	C(1)–Co(1)–C(16)	106.3(5)
C(2)–Co(1)–C(16)	98.0(5)	P(1)–Co(2)–C(11)	150.9(3)
P(1)–Co(2)–C(15)	110.9(3)	C(3)–Co(2)–C(4)	97.4(5)
C(3)–Co(2)–C(11)	100.3(4)	C(3)–Co(2)–C(15)	101.9(4)
C(4)–Co(2)–C(11)	104.8(4)	C(4)–Co(2)–C(15)	142.7(4)
C(11)–Co(2)–C(15)	40.6(4)	Co(1)–Co(3)–C(16)	50.4(3)
Co(2)–Co(3)–C(16)	73.5(3)	P(2)–Co(3)–C(5)	108.0(3)
P(2)–Co(3)–C(6)	103.7(4)	P(2)–Co(3)–C(16)	85.8(3)
C(5)–Co(3)–C(6)	96.3(5)	C(5)–Co(3)–C(16)	158.8(4)
C(6)–Co(3)–C(16)	95.8(4)	Co(1)–P(1)–Co(2)	71.7(1)
Co(1)–C(1)–O(1)	169(1)	Co(1)–C(2)–O(2)	174(1)
Co(2)–C(3)–O(3)	179(1)	Co(2)–C(4)–O(4)	176(1)
Co(3)–C(5)–O(5)	177(1)	Co(3)–C(6)–O(6)	176(1)

[a] Numbers in parentheses are estimated standard deviations the least significant digits.

C=C bond affords the saturated cluster **a**. Assuming that the coordinated olefinic bond in species **a** behaves similarly

Scheme I

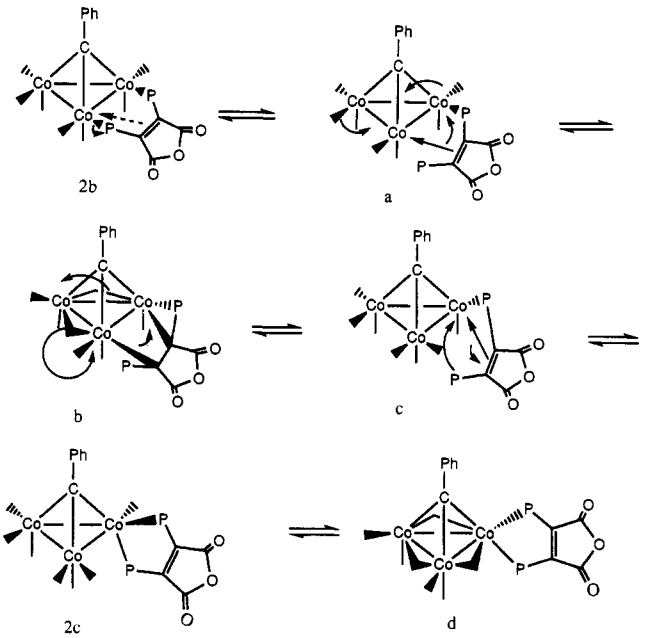

to a CO ligand in terms of migratory ability, an in-plane migration of two equatorial CO groups and the olefin moiety leads to cluster **b** with a bridging olefinic bond. Completion of the terminal-to-bridge ligand migration then yields the chelated alkenyl phosphine cluster **c**, which, upon olefin displacement by the free, dangling PPh_2 moiety, gives the chelated diphosphine cluster **2c**. It is this chelated isomer, with its axial and equatorial PPh_2 groups, that we observe in the low-temperature ^{31}P NMR spectra of **2**. The determined X-ray structure of **2** is produced by one last terminal/bridge exchange of the equatorial CO groups in **2c**.

The proposed bma ligand equilibration is consistent with the fact that terminal/bridge CO exchange is known to be facile in this genre of cluster and that the saturated diphosphine cluster $PhCCo_3(CO)_7$(dppe) does not exhibit such P-ligand movement.[24] Only the bridging isomer is observed since the requisite olefinic bond, which serves to tether the ligand to the cluster and preserves the electronic saturation at the cobalt centers in each of the intermediates, is absent.

The reactivity of **2** toward $P\text{–}C_{olefin}$ bond cleavage relative to that of the structurally similar cluster $PhCCo_3(CO)_7$(*cis*-$Ph_2PCH{=}CHPPh_2$) was investigated by independent thermolysis and photolysis experiments. When **2** was heated in THF solution at 43.6 °C, it was converted to **3** in >95% yield after 90 min ($t_{1/2}$ = ~18 min) while near-UV irradiation of **2** at 20 °C in THF solution gave **3** in quantitative yield. In contrast, when $PhCCo_3(CO)_7$(*cis*-$Ph_2PCH{=}CHPPh_2$) was heated overnight at 43.6 °C, no new cobalt carbonyl containing material was observed and the starting cluster was recovered in 64% yield. Photolysis led only to the complete decomposition of $PhCCo_3(CO)_7$(*cis*-$Ph_2PCH{=}CHPPh_2$). It is important that no P–C bond cleavage products of any kind were observed in either reaction. This suggests that if $P\text{–}C_{olefin}$ bond cleavage occurs, it is relatively inefficient in comparison to that of $PhCCo_3(CO)_7$(bma) and that the resulting product(s) must decompose before analysis.

Scheme II

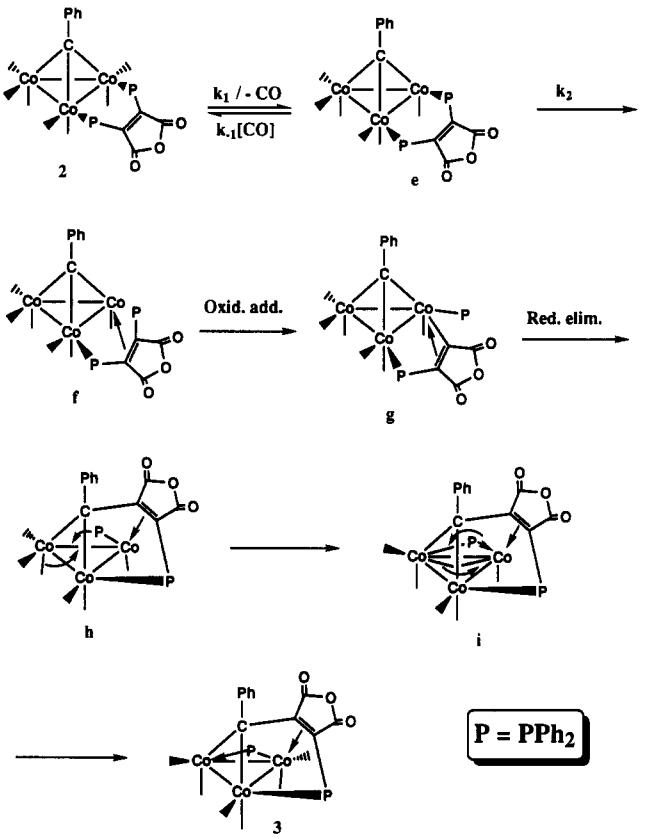

The formation of **3** from the bridging isomer of **2** is considered in Scheme II. As shown from the kinetic studies, dissociative CO loss from **2** represents the rate-determining step in the reactions leading to **3** and is expected to afford the unsaturated cluster **e**. We have shown the lost CO originating from a phosphine-substituted cobalt center.[27] Whether or not this is the initial site of CO loss is immaterial due to the rapid rates of intramolecular carbonyl scrambling in **2**, which would assist in the transfer of unsaturation to a bma-substituted cobalt atom.[28] Phosphine displacement by the noncoordinated C=C bond of the maleic anhydride ring would furnish species **f**. P–C_{olefin} bond oxidative addition yields the terminal phosphido cluster **g**, which is followed by a reductive elimination of the benzylidyne and (diphenylphosphido)maleic anhydride groups to give **h**.[29] The final product, cluster **3**, is obtained after a terminal-to-bridge conversion of the phosphido group that is coupled with the migration of a CO ligand from the lone $Co(CO)_3$ group to the adjacent olefin-substituted cobalt center.

The oxidative addition step is selective in that only the P–C_{olefin} bond is cleaved. No evidence for P–C_{aryl} bond cleavage was obtained. Our results are in keeping with the established reactivity trends concerning P–C bond scission; namely, electron-withdrawing substituents facilitate the cleavage of P–C bonds.[8a,10] In the case of cluster **2**, the more strongly electron-withdrawing maleic anhydride group is the preferred site for P–C bond scission.

Conclusions

The thermal reaction between $PhCCo_3(CO)_9$ and bma gives the new cluster $Co_3(CO)_6(\mu_2\text{-}\eta^2,\eta^1\text{-}C(Ph)C{=}C(PPh_2)C(O)OC(O))(\mu_2\text{-}PPh_2)$ without the spectroscopic observation of the expected diphosphine-substituted cluster $PhCCo_3(CO)_7$(bma). However, the independent synthesis of $PhCCo_3(CO)_7$(bma) has revealed that this cluster is, indeed, involved as a precursor to $Co_3(CO)_6(\mu_2\text{-}\eta^2,\eta^1\text{-}C(Ph)C{=}C(PPh_2)C(O)OC(O))(\mu_2\text{-}PPh_2)$. Kinetic studies on the conversion of **2** to **3** indicate that dissociative CO loss from cluster **2** is rate-limiting.

Both clusters have been characterized by solution methods and by X-ray crystallography. The bma ligand in cluster **2** exists in solution in both chelating and bridging forms, as shown by variable-temperature ^{31}P measurements. Cluster **2** with a bridging bma ligand is favored in solution at room temperature, but the preferred solid-state structure exhibits a chelating bma ligand. The fluxional behavior of the ancillary CO groups and the olefinic maleic anhydride bond undoubtedly assist in the equilibration of the bma ligand.

We plan to extend our studies to alkylidene-capped $RCCo_3(CO)_7$(bma) clusters and other isolobally related tetrahedrane clusters in order to probe the generality of bma ligand activation by P–C_{olefin} bond cleavage. These studies and the redox properties of clusters **2** and **3** will be reported in due course.

Experimental Section

General Procedures. $Co_2(CO)_8$ and 2,3-dichloromaleic anhydride were purchased from Pressure Chemical Co. and Aldrich Chemical Co., respectively. The Ph_2P(TMS) used in the synthesis of bma was prepared according to the published procedure.[30] $PhCCo_3(CO)_9$ was prepared by the procedure reported by Seyferth,[31] and the bma ligand was synthesized by using the method of Tyler.[12b] All reactions were carried out under argon using Schlenk techniques.[32] THF, 2,5-Me_2THF, and toluene were distilled from sodium/benzophenone ketyl while CH_2Cl_2 was distilled from CaH_2. All distilled solvents were stored under argon in Schlenk vessels equipped with Teflon stopcocks.

Infrared spectra were recorded on a Nicolet 20SXB FT-IR spectrometer. The ^{13}C and ^{31}P NMR spectra were recorded on a Varian 300-VXR spectrometer at 75 and 121 MHz, respectively. The reported ^{31}P chemical shifts are referenced to external H_3PO_4 (85%), taken to have $\delta = 0$. The positive chemical shifts are to low field of the external standard.

Synthesis of $PhCCo_3(CO)_7$(bma) (2). To a mixture of 0.2 g (0.39 mmol) of $PhCCo_3(CO)_9$ and 0.2 g (0.42 mmol) of bma in 20 mL of THF was added 0.06 g (0.80 mmol) of Me_3NO. The color of the solution changed from brown to green-black immediately. The reaction, which was monitored by IR, was complete after 0.5 h. The reaction

(27) Richmond, M. G.; Kochi, J. K. *Inorg. Chem.* **1986**, *25*, 1334.
(28) Intramolecular CO exchange in $PhCCo_3(CO)_7$(bma) is estimated to be 5×10^3 s^{-1} at room temperature.
(29) The reductive coupling of the μ_3-benzylidyne and the (diphenylphosphino)maleic anhydride ligands reported here is akin to the alkylidyne–alkyne coupling observed in other trinuclear clusters. See: (a) Churchill, M. R.; Ziller, J. W.; Shapley, J. R.; Yeh, W.-Y. *J. Organomet. Chem.* **1988**, *353*, 103. (b) Beanan, L. R.; Keister, J. B. *Organometallics* **1985**, *4*, 1713. (c) Lentz, D.; Michael-Schulz, H. *Inorg. Chem.* **1990**, *29*, 4396. (d) Nuel, D.; Dahan, F.; Mathieu, R. *J. Am. Chem. Soc.* **1985**, *107*, 1658.
(30) Kuchen, W.; Buchwald, H. *Chem. Ber.* **1959**, *92*, 227.
(31) Nestle, M. O.; Hallgren, J. E.; Seyferth, D. *Inorg. Synth.* **1980**, *20*, 226.
(32) Shriver, D. F. *The Manipulation of Air-Sensitive Compounds*; McGraw-Hill: New York, 1969.

solution was removed in vacuo at 0 °C, and $PhCCo_3(CO)_7$(bma) was isolated by column chromatography at −78 °C using CH_2Cl_2/petroleum ether (1:1). Yield: 0.25 g (70%). A sample of **2** was not submitted for combustion analysis due to the facile loss of CO. IR (CH_2Cl_2): ν(CO) 2065 (s), 2015 (s), 1986 (sh), 1824 (w, asym bma C=O), 1772 (m, sym bma C=O) cm^{-1}. $^{31}P\{^1H\}$ NMR (THF, −97 °C): δ 62 (chelate), 54 (chelate), 37 (bridge). $^{13}C\{^1H\}$ NMR (THF, −97 °C): δ 209 (2C, bridge), 207 (chelate), 204 (2C, bridge), 202 (3C, bridge).

Synthesis of $Co_3(CO)_6(\mu_2\text{-}\eta^2,\eta^1\text{-}C(Ph)C{=}C(PPh_2)C(O)OC(O))(\mu_2\text{-}PPh_2)$ (3). To 0.5 g (0.96 mmol) of $PhCCo_3(CO)_9$ and 0.47 g (1.0 mmol) of bma was added 50 mL of toluene, after which the solution was heated at 75 °C overnight. Upon cooling, TLC analysis revealed the presence of the desired products along with a trace of the parent cluster. Cluster **3** was subsequently isolated by column chromatography on silica gel using CH_2Cl_2 as the eluant. Analytically pure $Co_3(CO)_6(\mu_2\text{-}\eta^2,\eta^1\text{-}C(Ph)C{=}C(PPh_2)C(O)OC(O))(\mu_2\text{-}PPh_2)$ was obtained by recrystallization from benzene/isooctane (1:1). Yield: 0.5 g (58%). IR (CH_2Cl_2): ν(CO) 2062 (m), 2042 (vs), 2025 (vs), 2010 (sh), 1939 (b, m), 1811 (m, asym bma C=O), 1748 (m, sym bma C=O) cm^{-1}. $^{31}P\{^1H\}$ NMR (THF, −97 °C): δ 201 (μ_2-phosphido), 12 (phosphine). $^{13}C\{^1H\}$ NMR (THF, −97 °C): δ 210.5 (1C, $J_{P\text{-}C}$ = 12.3 Hz), 202.9 (1C, $J_{P\text{-}C}$ = 7.9 Hz), 202.5 (1C), 201.9 (1C), 197.0 (1C), 192.8 (1C). Anal. Calcd (found) for $C_{41}H_{25}Co_3O_9P_2$: C, 54.69 (54.55); H, 2.80 (2.88).

X-ray Diffraction Structure of $PhCCo_3(CO)_7$(bma). A dark green-black crystal, which was grown from a CH_2Cl_2 solution of **2** that had been layered with heptane, of dimensions 0.04 × 0.42 × 0.10 mm was sealed inside a Lindemann capillary, which was mounted on the goniometer of an Enraf-Nonius CAD-4 diffractometer. The radiation used was Mo Kα monochromatized by a crystal of graphite. Cell constants were obtained from a least-squares refinement of 25 reflections with $2\theta > 28°$. Intensity data in the range $2.0 \le 2\theta \le 40.0°$ were collected at 298 K using the ω-scan technique in the variable-scan speed mode and were corrected for Lorentz, polarization, and absorption (DIFABS). Three reflections (800, 080, 00$\bar{6}$) were measured after every 3600 s of exposure time in order to monitor crystal decay (<2%). The structure was solved by SHELX-86, which revealed the positions of the Co and P atoms. All remaining non-hydrogen atoms were located with difference Fourier maps and blocked-matrix least-squares refinement. With the exception of the phenyl and CO carbons, all non-hydrogen atoms were refined anisotropically. Refinement converged at R = 0.0367 and R_w = 0.0391 for 1344 unique reflections with $I > 3\sigma(I)$.

X-ray Diffraction Structure of $Co_3(CO)_6(\mu_2\text{-}\eta^2,\eta^1\text{-}C(Ph)C{=}C(PPh_2)C(O)OC(O))(\mu_2\text{-}PPh_2)$. Single crystals for crystallographic analysis were grown from a CH_2Cl_2 solution of **3** that had been layered with heptane. A suitable black crystal of dimensions 0.05 × 0.05 × 0.52 mm was selected and sealed inside a Lindemann capillary, which was mounted on the goniometer of an Enraf-Nonius CAD-4 diffractometer employing Mo Kα radiation. Cell constants were obtained from a least-squares refinement of 25 reflections with $2\theta > 25°$. Intensity data in the range $2.0 \le 2\theta \le 44.0°$ were collected at 298 K using the ω-scan technique in the variable-scan speed mode and were corrected for Lorentz, polarization, and absorption (DIFABS). Three reflections (600, 080, 0,0,12) were measured after every 3600 s of exposure time in order to monitor crystal decay (<1%). The structure was solved by MULTAN, which revealed the positions of the Co and P atoms. All remaining non-hydrogen atoms were located with difference Fourier maps and least-squares refinement. With the exception of the phenyl carbons, all non-hydrogen atoms were refined anisotropically. Refinement converged at R = 0.0392 and R_w = 0.0432 for 2012 unique reflections with $I > 3\sigma(I)$.

Kinetic Studies. All kinetic reactions were conducted in Schlenk tubes and monitored for a minimum of 2–3 half-lives by following the IR absorbance of the 1772-cm^{-1} carbonyl band of **2**. Plots of ln A_t vs time gave the first-order rate constants listed in Table I. The activation parameters ($\Delta H^\ddagger$ and $\Delta S^\ddagger$) were determined by using the Eyring equation, and error limits were calculated by using the available least-squares regression program.[33]

Acknowledgment. We thank Ken Wegner for recording the NMR spectra. Financial support from the Robert A. Welch Foundation (Grants B-1202-SGB and B-1039-MGR) and the UNT Faculty Research Program is gratefully acknowledged.

Supplementary Material Available: Textual presentations of the crystallographic experimental details and listings of crystallographic data, bond distances, bond angles, anisotropic thermal parameters, and hydrogen positional parameters for $PhCCo_3(CO)_7$(bma) and $Co_3(CO)_6(\mu_2\text{-}\eta^2,\eta^1\text{-}C(Ph)C{=}C(PPh_2)C(O)OC(O))(\mu_2\text{-}PPh_2)$ (28 pages). Ordering information is given on any current masthead page.

OM930458S

(33) Gordon, A. J.; Ford, R. A. *The Chemist's Companion*; Wiley-Interscience: New York, 1972.